

An Innovative and Viable Route for the Realization of Ultra-Thin Supercapacitors Electrodes Assembled with Carbon Nanotubes

Z. D. Kovalyuk¹, F. V. Motsnyi², O. S. Zinets³, S. P. Yurcenyuk¹, E. Tamburri^{4,*}, S. Orlanducci⁴, V. Guglielmotti⁴, F. Toschi⁴, M. L. Terranova⁴, and M. Rossi⁵

¹Chernivtsi Department of Institute for Problem of Materials Science, National Academy of Sciences of Ukraine, 5, I. Vilde Street, 58001 Chernivtsi, Ukraine

²V. Lashkaryov Institute of Semiconductor Physics, National Academy of Sciences of Ukraine, 41 Prospect Nauky, 03028 Kyiv, Ukraine

³Institute for Nuclear Research, National Academy of Sciences of Ukraine, 47 Prospect Nauky, 03028 Kyiv, Ukraine

⁴Dipartimento di Scienze e Tecnologie Chimiche, MINASlab, Università di Roma Tor Vergata, Via della Ricerca Scientifica, 00133 Roma, Italy

⁵Dipartimento di Energetica, Università di Roma Sapienza, Via A. Scarpa 16, 00161 Roma, Italy

Electrochemical Double Layer Capacitors (EDLC), also known as supercapacitors, have been fabricated using Single Walled Carbon Nanotubes (SWCNTs) as active material for electrode assembling. In particular a new way of fabrication of ultra-thin electrodes ($\leq 25 \mu\text{m}$) directly formed on the separator has been proposed, and a prototype of EDLC has been realized and tested. For such devices the specific capacitance is in the range 40–45 F/g and the internal resistances in the range 6–8 $\Omega \cdot \text{cm}^2$, at current density of 2 $\text{mA} \cdot \text{cm}^{-2}$.

Keywords: Carbon Nanotube, Supercapacitor, Thin Electrode, Capacitance.

1. INTRODUCTION

One of important applications of nanocomposite carbon-based structures and of carbon nanotubes (CNT) is their use as anodes in lithium-ion batteries and electrodes for electrochemical capacitors with a high-specific capacity.^{1,2} In Electrochemical Double Layer Capacitors (EDLC) the stored energy is based on the separation of charged species across the electrode/electrolyte interface. Positive and negative electrodes are typically made from high surface area carbon materials immersed in an electrolyte solution. By either increasing the size of the electrode/electrolyte interface, thus increasing the surface area of the electrodes, or decreasing the separation between ions and electrode, the stored capacitance increases. Therefore, for the realization of the electrodes, the use of CNT, material characterized by a very high specific surface area ($\sim 600 \text{ m}^2 \text{ g}^{-1}$ or more) and exceptional conducting and mechanical properties, is expected to improve the performances of the devices.^{3–5} Recently, many researches have been focused to

the production of carbon nanotubes based electrodes with high performances. These include, for example, the realization of composite electrodes made of carbon nanotubes and conducting polymers.^{6–8} In these systems the energy stored in the capacitor is either capacitive or pseudocapacitive, owing to the increased specific surface area of the composite material and to the Faradic redox reactions that occur within the conducting polymer matrix. Moreover the introduction of CNT into polymers improves their electric conductivity and mechanical properties.⁹ Other studies have been addressed to the realization of hybrid electrodes by coupling carbon nanotubes with inorganic species such as metals, metal oxides and metal hydroxides.^{10–12} The aim of such investigations was again to improve the specific capacitance of the final supercapacitor by matching two electrode materials with different charge-storage mechanism in one composite electrode.

Anyway, EDLC performances are affected by a number of factors such as pore size, surface area, surface chemistry and graphitization of the electrode material. A key role is moreover played by the electrode thickness.^{2–4, 13–14} This last point is connected with the process of the separation

*Author to whom correspondence should be addressed.

of active material particles from the geometrical surface of an electrode that directly contacts the electrolyte, into the depth of the electrode. This effect increases the internal resistance of capacitors. Moreover remoteness of the active material particles from the current collector also results in an increase of the internal resistance of the supercapacitor. Taking into account these factors, it appears that a viable solution is the use of ultra-thin electrodes with a thickness comparable to the size of the active material grains. In practice, however, the formation of such ultra-thin electrodes meets significant technological difficulties.

We have developed a new methodology for the formation of ultra-thin electrodes directly on the supercapacitor separators, using the same type of single-walled carbon nanotubes (SWCNT) investigated in a previous paper.¹⁵ In the present paper the fabrication of electrodes using SWCNTs is described and the charge–discharge characteristics of the supercapacitors are reported and discussed.

2. EXPERIMENTAL DETAILS

2.1. Fabrication of Electrodes

Samples of commercial SWCNTs produced by arc-discharge are treated following the protocols described in Ref. [16]. The final amount of nickel in the purified material is about 3.2%. The electrolyte is a 30% w/w KOH water solution. The SWCNTs suspension is prepared by adding carbon nanotubes to the electrolyte solution. This suspension is then transferred on the separator material by spraying or drop casting. Materials “BAKHIT” and non-woven polypropylene or CELGARD are used as separators. The separator is placed over two or three layers of a filtering paper which is properly humidified in order to produce a good mechanical contact. The dispersion’s solvent soaks up by the bottom layers of the filtering paper and the SWCNTs create a rather uniform thin layer on the surface of the separator, which is finally used as electrode of the supercapacitor.

2.2. Characterization of Electrodes

Surface morphologies of electrode were examined using a field emission scanning electron microscope (FE-SEM, HITACHI S-4000) operating at an acceleration voltage of 20 kV.

Electrochemical measurements were performed by means of an electrochemical workstation using two-electrode electrochemical capacitor cells and a three-electrode system in 30% w/w KOH aqueous solution. In the three electrode system the SWCNTs ultra-thin layer was used as working electrode, whereas a platinum wire and a saturated calomel electrode (SCE) were used as the counter and reference electrodes, respectively.

The SWCNTs electrodes performances were tested using the following techniques: cyclic voltammetry in

the range of potential between -1.14 and $+0.80$ V at scan rates from 5 to 50 mVs^{-1} , galvanostatic charging–discharging (current ranges 1–5 mA) and AC impedance spectroscopy using the AC amplitude of 10 mV in the frequency range from 1 mHz to 100 kHz.

3. RESULTS AND DISCUSSION

3.1. Morphological Characteristics of Electrodes

Figure 1 shows a FE-SEM image of a typical SWCNTs-coated electrode surface. The entangled carbon nanotube bundles form net-like systems characterized by high porosity. The produced electrodes have a geometrical surface S of about 0.5 cm^2 .

The layer thickness d is evaluated using the following equation:

$$d = \frac{Nm}{\rho_{\text{sph}} \cdot S} \quad (1)$$

where m is the amount of the SWCNTs suspension, N is the SWCNTs weight concentration of the suspension, S is the geometrical surface of electrode and ρ_{sph} is the particles density calculated using the Smoothed Particle Hydrodynamics method.¹⁷ Such an approach allows us to take into account the spatial distribution assumed by a highly porous system produced from evaporation of a fluid in which particles have been properly dispersed. In this way, it is possible to estimate a d value that is reasonably more realistic than the one obtained using the theoretical density of carbon nanotubes. For our electrodes we estimated a thickness d ranging between 15 and 18 μm .

In order to verify these data, the layer thickness d has been evaluated by profilometer surface measurements. These analyses provide d values in the range 15–25 μm . Nevertheless, it must consider that such measurements suffer of severe uncertainties, due to the highly porous nature of the surfaces. Moreover, the deposition technique also influences the uniformity of the layer, that strongly

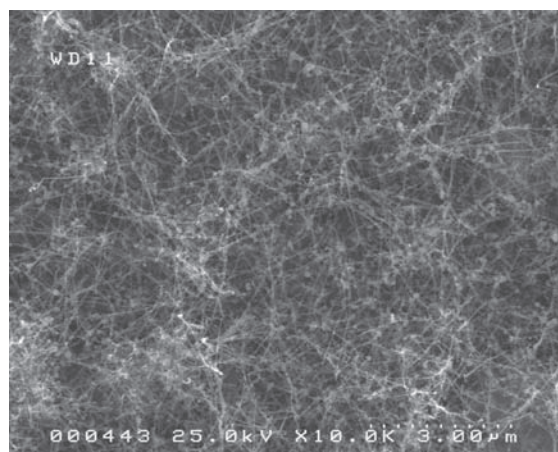


Fig. 1. FE-SEM image of a SWCNTs ultra-thin layer surface.

depends on the kind of separator and, in particular, on its structure and pore size. In particular we found that for the layers deposited by spraying the non-uniformity of the thickness does not exceed 20–25% for the separator material of type “BAKHIT” and nonwoven polypropylene; and 12–17% for the material CELGARD. For layers deposited by the drop method these values are increased by 4–8% in the case of CELGARD material and approximately by 10% in the case of “BAKHIT” and nonwoven polypropylene.

On the basis of such considerations, it is realistic to assume a thickness $\leq 25 \mu\text{m}$ for all our SWCNTs electrodes.

3.2. Electrodes Characterization

Figure 2 shows a typical cyclic voltammogram obtained for the SWCNTs electrodes in 30% w/w KOH water solution in the potential range $(-1.14 \div +0.80)$ V. The rectangular-like form (close to that of an ideal capacitor) and the absence of peaks in the voltammogram evidence the absence of faradic reactions, representing one of the necessary conditions for effective energy storage in the double electric layer.

The dependence of the imaginary part of impedance versus its real part for the same electrode is reported in Figure 3. Using this plot it is possible to calculate the internal resistance and the equivalent scheme needed for evaluation of the specific power and for comparison with the performances of other supercapacitors.

3.3. Charge–Discharge Characteristics of Supercapacitors

Charge–discharge characteristics of the supercapacitors were measured in galvanostatic mode at the limit charge voltage of 1 V. The voltage was limited by the use of the KOH aqueous electrolyte solution.

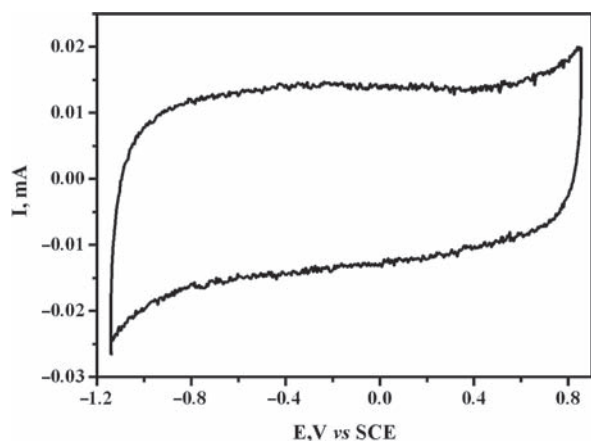


Fig. 2. Cyclic voltammogram of SWCNTs electrodes in 30% w/w KOH aqueous solution in range of potential $(-1.14 \div 0.80)$ V at 50 mVs^{-1} .

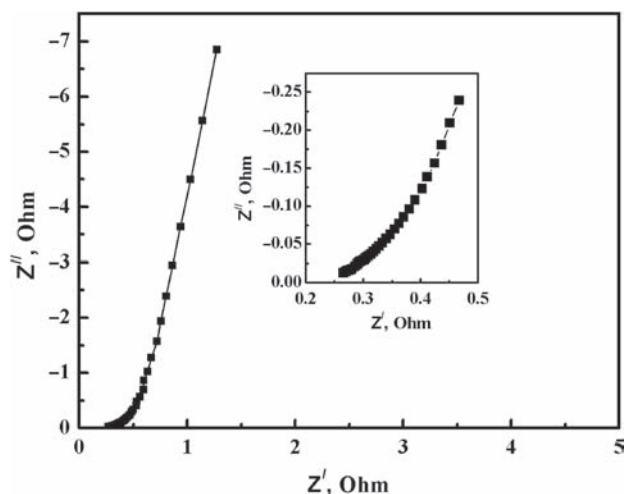


Fig. 3. Measured electrochemical impedance plot for a typical SWCNTs electrode in 30% w/w KOH aqueous solution. The inset evidences the details of the impedance curve at low values.

Figure 4 presents the typical discharge curves at different resistance loads of the SWCNTs based supercapacitors. Capacitors were charged under the following conditions: the charge current was $I_c^1 = 5 \text{ mA}$ up to the capacitor voltage 0.9 V and $I_c^2 = 1 \text{ mA}$ up to the end capacitor voltage 0.95 V . The end voltage under discharge was 0.05 V .

Figure 5 presents curves of the charge–discharge cycles when the $C_d/C_c \approx 1$ (C_d and C_c are the discharge and the charge capacity, respectively) in galvanostatic mode ($I_{c-d} = \text{const} = 1 \text{ mA}$). At the beginning, the ratio C_d/C_c was in the range $0.7\text{--}0.9$ for all the produced EDLC, but depending on the supercapacitors this ratio was found to reach the unity after a different number of cycles, $10\text{--}20$ or $70\text{--}90$ cycles. These different performances of the fabricated devices may be explained on the basis of electrochemical reactions at the electrodes and of the inertia of the electric double-layer formation, ascribed to the presence of impurities in electrolytes.

The specific capacitance of electrodes was in the range $40\text{--}45 \text{ F/g}$. The internal resistance of the supercapacitors equals $\sim 6\text{--}8 \text{ Ohm}\cdot\text{cm}^2$ at the current density of 2 mA/cm^2 .

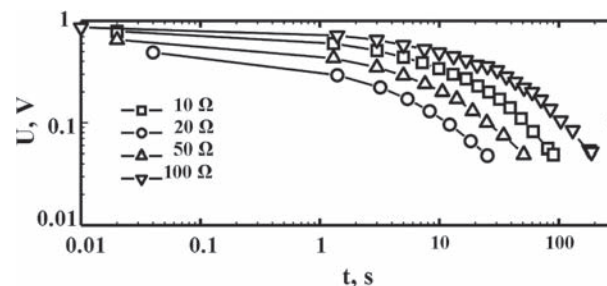


Fig. 4. Chronopotentiometry curves at resistance loads ranging from 10 to 100Ω in 30% w/w KOH aqueous solution for supercapacitors fabricated using SWCNTs-based electrodes and charged with a charge current of 1 mA .

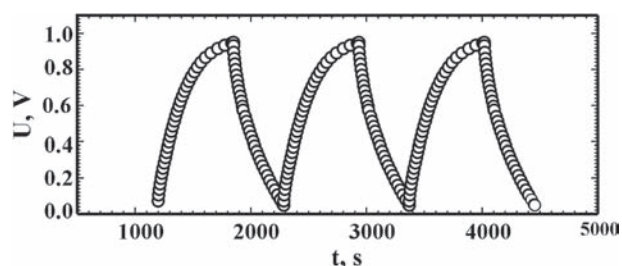


Fig. 5. Charge–discharge cycles measured for SWCNTs-based supercapacitors at charge–discharge current of $I_{c-d} = 1$ mA in 30% w/w KOH aqueous solution when $C_d/C_c \approx 1$.

The charge–discharge behavior reported in Figure 5 is similar to those observed in Refs. [4, 5]. According to Ragone's diagram,^{18–19} values of 40–45 F/g and internal resistance of $\sim 0.2 \Omega \text{ cm}^2$ would correspond to a specific power of 5–5.1 Wh/kg. The higher internal resistance measured in our experiments could be caused by imperfection of the electric contacts between the electrode material and the current collector surface due to the electrode surface relieves. Due to feature of the nanotubes deposit on the separator, electric contact of electrode-current collector occurs through local dots formed by SWCNTs aggregates. Hence, the contact surface area is very small. On the other hand, imperfect electric contact between the nanotubes in the electrode material also leads to increase the supercapacitor internal resistance. An upgrading of the fabrication strategies, leading to a better distribution of the nanotubes on the electrode and to the realization of more efficient conducting networks is needed in order to overcome these problems.

Anyway the values of specific capacitance found for our SWCNTs electrodes are very encouraging being higher of the typical values (in the range 20–25 F/g) measured for electrodes made solely by carbon nanotubes and used as components of more complex devices.^{11–12}

Finally, in order to better define the functional applications of our SWCNTs-based supercapacitors, we checked the specific capacitance dependence on the frequency. Figure 6 evidences that the specific capacitance decrease with the frequency. The high capacitance values obtained at frequencies below 0.01 Hz indicates the advantage to use such supercapacitors, for instance, as devices for energy storage working in a constant current mode.

4. CONCLUSIONS

A new route for the fabrication of ultra-thin ($\leq 25 \mu\text{m}$) supercapacitor electrodes that use only single-walled carbon nanotubes as active material has been settled.

The electrodes are formed directly on the separator of the supercapacitor cell. The internal resistance of the fabricated supercapacitors is in the range $6\text{--}8 \Omega \times \text{cm}^2$ at the current density 2 mA/cm^2 and specific capacitances in the range 40–45 F/g have been measured with electrode thickness in the range 15–25 μm .

The material results stable under prolonged cycling and the type of device assure intrinsically long operational life, requiring basically no maintenance. Another advantage of this innovative supercapacitor technology is the easy fabrication and the profitable scaling-up.

The supercapacitors based on SWCNTs and realized following this operational route result particularly advantageous for the use as energy accumulator at low frequencies and could constitute the base material for the realization of high performance electrode materials.

References and Notes

1. R. H. Xie, J. Zhao, and Q. Rao, *Encyclopedia of Nanoscience and Nanotechnology*, edited by H. S. Nalwa, ASP, USA (2004), Vol. X, p. 1.
2. H. J. In, S. Kumar, Y. Shao-Horn, and G. Barbastathis, *Appl. Phys. Lett.* 88, 083104 (2006).
3. K. H. An, K. K. Jeon, J. K. Heo, S. C. Lim, D. J. Bae, and Y. H. Lee, *J. Electrochem. Soc.* 149, A1058 (2002).
4. E. Frackowiak, *J. Braz. Chem. Soc.* 17, 1074 (2006).
5. A. B. Fuertes, G. Lota, T. Centeno, and E. Frackowiak, *Electrochim. Acta* 50, 2799 (2005).
6. J. Wang, Y. Xu, X. Chen, and X. Sun, *Compos. Sci. Tech.* 67, 2981 (2007).
7. J. Y. Kim, K. H. Kim, and K. B. Kim, *J. Power Sources* 176, 396 (2008).
8. X. Lin and Y. Xu, *Electrochim. Acta* 53, 4990 (2008).
9. M. Moniruzzaman and K. I. Winey, *Macromol.* 39, 5194 (2006).
10. C. T. Hsieh, Y. W. Chou, and W. Y. Chen, *J. Solid State Electrochem.* 12, 663 (2008).
11. L. Su, X. Zhang, C. Yuan, and B. Gao, *J. Electrochem. Soc.* 155, A110 (2008).
12. M. Skunik, M. Chojak, I. A. Rutkowska, and P. J. Kulesza, *Electrochim. Acta* 53, 3862 (2008).
13. E. Rajmundo-Pinero, D. Cazorla-Amoros, A. Linares-Solano, S. Delpeux, E. Frackowiak, K. Szostak, and F. Béguin, *Carbon* 40, 1597 (2002).
14. C. Largeot, C. Portet, J. Chmiola, P. L. Taberna, Y. Gogotsi, and P. Simon, *J. Am. Chem. Soc.* 130, 2730 (2008).
15. A. A. Konchits, F. V. Motsnyi, Yu. N. Petrov, S. P. Kolesnik, V. S. Yefanov, M. L. Terranova, E. Tamburri, S. Orlanducci, V. Sessa, and M. Rossi, *J. Appl. Phys.* 100, 124315 (2006).
16. M. L. Terranova, S. Orlanducci, E. Fazi, V. Sessa, S. Piccirillo, M. Rossi, D. Manno, and A. Serra, *Chem. Phys. Lett.* 381, 86 (2003).
17. J. J. Monaghan, *Rep. Prog. Phys.* 68, 1703 (2005).
18. R. Kötz and M. Carlen, *Electrochim. Acta* 45, 2483 (2000).
19. S. Arepalli, H. Fireman, C. Huffman, P. Moloney, P. Nikolaev, L. Yowell, C. D. Higgins, K. Kim, P. A. Kohl, S. P. Turano, and W. J. Ready, *JOM* 57, 26 (2005).

Received: 5 March 2008. Accepted: 24 April 2008.